

Dynamic Mechanical Thermal Analysis of Thermally Stable and Thermally Reactive Network Polymers

W. D. Cook, T. F. Scott, S. Quay-Thevenon, J. S. Forsythe

School of Physics and Materials Engineering, Monash University, PO Box 69M Victoria 3800, Australia

Received 13 December 2003; accepted 11 January 2004

DOI 10.1002/app.20569

Published online in Wiley InterScience (www.interscience.wiley.com).

ABSTRACT: The temperature and frequency dependence of the dynamic mechanical properties in the glass transition was studied for a series of partially cured thermally reactive networks (low temperature cured epoxy and a dimethacrylate photocured with a conventional initiator) and more thermally stable networks (high temperature cured epoxy and two dimethacrylates photocured with a photoinitiator). The viscoelastic behavior in the transition region of the former networks changed during the experiment due to additional cure, whereas the thermally stable networks enabled the study of the effect of conversion on the transition region. The glass transition temperatures showed 1 : 1 rela-

tionships with the isothermal curing temperatures and were correlated with the degree of conversion. The breadth of the glass transition, as determined from the real and loss moduli, $\tan \delta$, and the loss compliance in the temperature and frequency domains, was found to be greater for the dimethacrylate networks than for the epoxy networks. The breadth of the transition for the dimethacrylates was not significantly dependent on the degree of cure. © 2004 Wiley Periodicals, Inc. *J Appl Polym Sci* 93: 1348–1359, 2004

Key words: DMTA; glass transition; networks; partial cure; epoxy; dimethacrylate; transition breadth

INTRODUCTION

All amorphous materials exhibit a glass transition that marks the change from a glassy state to a liquidlike state. The glass transition temperature (T_g) is one of the most important parameters of a polymer, as it determines the maximum use temperature (for glasses) and the minimum use temperature (for rubbers). In addition, the T_g determines the minimum polymerization temperature that can be employed for full conversion to polymer. However, the glass transition does not really occur at a specific temperature but moreover in a temperature range. Thus, the performance of a polymer is also dependent on the breadth of the transition so that, for example, a broader transition results in a higher heat distortion temperature.¹

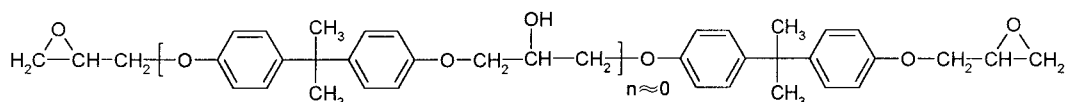
When a thermosetting resin cures, the molecular motions start to become restricted, and as this proceeds, the material may vitrify during the cure,^{2–6} which freezes in the molecular mobility and prevents further reaction, possibly leading to inferior thermal and mechanical properties. Therefore, it is important to understand how the viscoelastic properties of a thermoset vary with the extent of cure. In addition, it has been argued^{7–11} that some thermo-

sets have a heterogeneous structure with regions of low and high crosslink densities and this may affect their ultimate properties. Because the breadth of the glass transition region gives an indication of the range of molecular mobilities in the network, studies of the glass transition can provide information about heterogeneity.

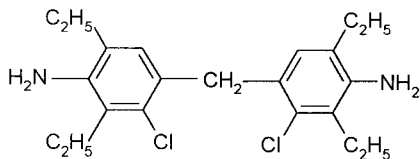
If the partly cured, but vitrified, sample is subsequently temperature-ramped in a dynamic mechanical thermal analysis (DMTA) experiment, the material will initially be in the glassy state and, therefore, be incapable of reacting until the scanning temperature is in the vicinity of the glass transition temperature of the partially cured resin. As the temperature is increased further, the molecular segments will become more mobile, allowing the reactive sites to recommence polymerization^{2,4–6,12}; this process significantly affects the measured DMTA spectrum.^{2,5,12}

In this article, we investigate the variation in dynamic mechanical properties in the glass transition region for two conventional networks that continue to crosslink during the experiment, and for two other systems that seek to avoid this problem. One of the conventional networks is a thermally cured, high-reactivity aromatic amine-epoxy system. Due to the rigidity of the structure and the reactivity of the functional groups, this system polymerizes at a measurable rate in the same temperature region as the glass transition of the partially cured network. The second system is a dimethacrylate that is photopolymerized by a conventional photoinitiator that

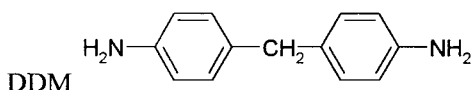
Correspondence to: W. D. Cook (wayne.cook@spme.monash.edu.au).



DGEBA



MCDEA

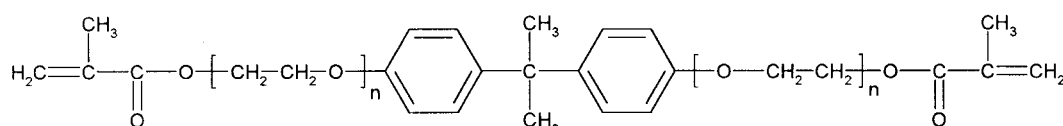
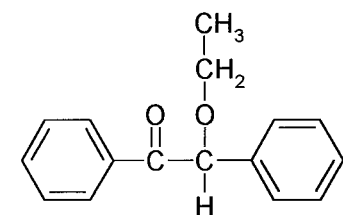


DDM

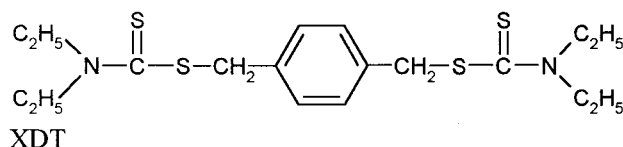
Scheme 1 Structures of the epoxy and amine curatives.

produces radicals which can be trapped in a vitrifying matrix but which are mobilized when the temperature is raised above the T_g . Both of these systems lead to complications in the interpretation of the DMTA behavior of the partly cured network because the network structure continues to develop during the thermal analysis experiment.¹³ The third network is an epoxy cured by an aromatic amine which has very low reactivity due to the presence of electron withdrawing groups and sterically restrictive groups on the benzene ring.¹⁴ In this case, the system polymerizes slowly only at temperatures close to the glass transition of the partially cured

network. The fourth system uses a xylylene diethyldithiocarbamate photoinitiator, which acts as a radical initiator and a chain terminator.^{15,16} During irradiation, the photoinitiator produces a carbon-centered radical and a sulfur-centered dithiocarbamyl radical but only the former can initiate polymerization.^{15,16} When the irradiation is terminated, the propagating radical is capped by one of the mobile dithiocarbamyl radical fragments, forming a thermally stable species.¹⁷ Thus, the use of photoinitiators conveniently allows for the examination of the network properties without inadvertently postcuring the sample when it is heated above its T_g .

 $n = 1$ DEBPADMA, $n=2$ TEBPADMA

BEE



XDT

Scheme 2 Structures of the dimethacrylates and photoinitiators.

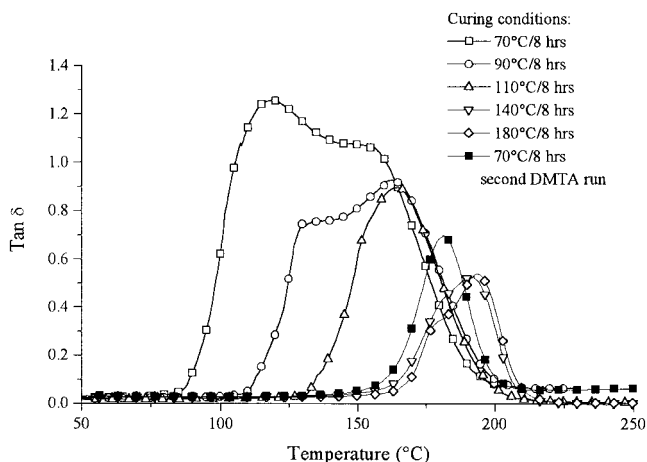


Figure 1 $\tan \delta$ versus temperature for DGEBA/DDM cured for 8 h at different temperatures. The conversion of epoxy groups before the DMTA run was 84, 86, 95, 97, 98, and 98% for the samples cured at 70, 90, 110, 140, and 180°C, respectively, and for a sample cured at 70°C for 8 h and temperature scanned in the DMTA (to 250°C) before rerunning, respectively.

EXPERIMENTAL

Materials

Two network types were studied—step-growth polymerized epoxies and radical cured dimethacrylates. The epoxy was the diglycidyl ether of bisphenol-A (DGEBA, supplied by Dow Chemicals; see Scheme 1) and had an epoxy equivalent of 189 g/mol (based on the manufacturer's data). The DGEBA was cured with either 4,4'-methylenebis(3-chloro-2,6-diethylaniline) (MCDEA; supplied by Aldrich; see Scheme 1) or diaminodiphenyl methane (DDM; supplied by Aldrich; see Scheme 1). The DGEBA/diamine samples were prepared by melting the diamine above its melting

point (90°C for MCDEA and 100°C for DDM) and quickly mixing it with the stoichiometric amount of the DGEBA (also heated at the same temperature). The mixture was then quickly cooled to minimize reaction.

Two dimethacrylates were also used in the study: a diethoxylated bisphenol-A dimethacrylate (DEBPADMA; supplied by Sartomer as SR348; see Scheme 2) and a tetraethoxylated bisphenol-A dimethacrylate (TEBPADMA; supplied by SARTOMER as CD540; see Scheme 2). Two photoinitiators were used to polymerize the dimethacrylates—0.5 wt % of a conventional initiator, benzoin ethyl ether (BEE; supplied by Aldrich; see Scheme 2) and 0.2 wt % of an initer photoinitiator, *p*-xylylene diethyldithiocarbamate (XDT; see Scheme 2 and synthesized as described previously¹⁸ according to the method of Otsu and Kuriyama¹⁹).

DMTA samples were produced by injecting the resin in a mold composed of two glass slides and PET release film separated by a silicone spacer. The thickness of the samples was approximately 2 mm. The dimethacrylate mixtures were photocured at a range of temperatures and times with a Spectroline UV lamp (Model SB-100P/F), which had an intensity of 4.2 mW/cm² at 365 nm on the top face of the sample.¹⁸ The photocured samples were placed on a thermally controlled aluminium platform and allowed to equilibrate before irradiation. The epoxy specimens were prepared at the stoichiometric ratio and were cured by using a range of temperatures and times. Near-infrared spectra with a resolution of 4 cm⁻¹ were recorded for all samples before and after cure by using a Perkin-Elmer GX NIR spectrometer. Coaddition of 16 scans was performed for each measurement. The conversion of the dimethacrylate groups was determined from the ratio of the peak areas of the methacrylate band²⁰ at 6166 cm⁻¹ before and after cure. The conversion of the epoxy groups was determined from the

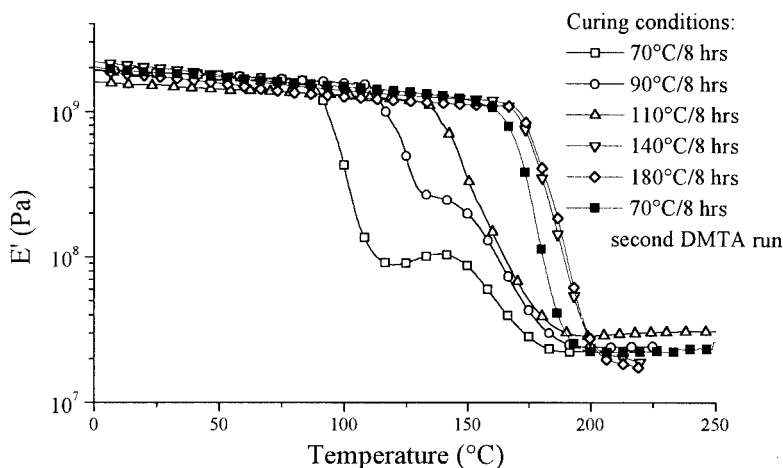


Figure 2 Real modulus versus temperature for partly and fully cure DGEBA/DDM. The conversion of epoxy groups before the DMTA run was 84, 86, 95, 97, 98, and 98% for the samples cured at 70, 90, 110, 140, and 180°C, respectively, and for a sample cured at 70°C for 8 h and temperature scanned in the DMTA (to 250°C) before rerunning, respectively.

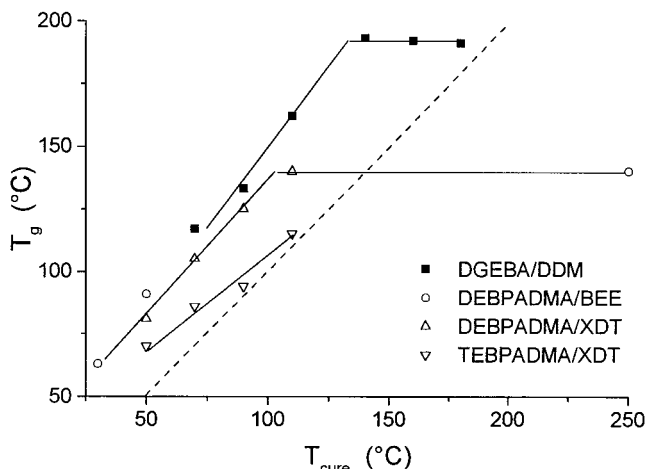


Figure 3 Dependence of T_g on cure temperature for networks that had vitrified during cure. The dashed line represents a 1 : 1 ratio.

ratios of the heights of the oxirane ring combination band²¹ at 4528 cm^{-1} before and after cure (peak areas were not used in this instance because of some overlapping at the edges of the absorption). Both epoxy and dimethacrylate spectra were normalized by using the aromatic ring C—H stretch combination band²¹ at 4620 cm^{-1} .

The dynamic mechanical behavior was determined by use of a Rheometric Scientific DMTA IV scanning at $2^\circ\text{C}/\text{min}$ at 1 Hz with a 0.1% strain, in a dual cantilever configuration. The storage modulus (E'), loss modulus (E''), and $\tan \delta$ were measured through the transition from the glassy to the rubbery state. The T_g was taken at the maximum of the $\tan \delta$ curve in the glass transition region at 1 Hz. The breadth of the glass transition of the $\tan \delta$ curve was determined as the full-width at half-maximum (FWHM). Multifrequency

experiments were also performed at 10 different frequencies between 0.1 and 20 Hz in 5°C temperature intervals and time-temperature superposition (TTS) was performed by using the Rheometric Scientific Orchestrator software, Version 6.5.7. The superposition was based on the E' data by using the T_g as the reference temperature. The superposition shift factors were fitted over the transition region by using the Williams-Landel-Ferry (WLF) equation²²

$$\log_{10} a_T = \frac{-C_1(T - T_g)}{C_2 + T - T_g} \quad (1)$$

where a_T is the horizontal shift factor (as determined using TTS) and T is the temperature of the shifted data.

Another measure of the range of relaxation times was obtained by fitting the superposed real modulus (E') data to the stretched exponential expression

$$E' = E_0 e^{-(1/\omega\tau)^n} + E_\infty \quad (2)$$

where E_0 and E_∞ are the unrelaxed (glassy) and relaxed (rubbery) moduli, ω is the frequency, τ is the relaxation time, and the exponent n is the distribution parameter. This equation was adapted from the William-Watts equation²³ for the stress relaxation modulus on the basis that $E(t) \approx E'(\omega)$ at $\omega = 1/t$. This approximation was also used by Kannurpatti et al.¹³ and is valid provided that the distribution of relaxation times is broad.²⁴

RESULTS AND DISCUSSION

Networks formed by step growth polymerization

The dynamic mechanical properties of DGEBA/DDM samples cured for 8 h at various temperatures are

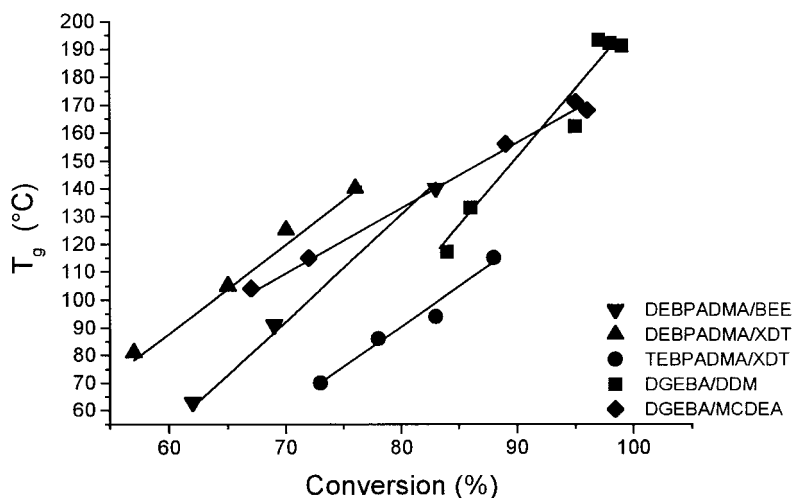


Figure 4 T_g versus conversion for partially cured DGEBA/MCDEA, DGEBA/DDM, DEBPADMA, and TEBPADMA

shown in Figures 1 and 2. Based on earlier studies of the kinetics of these systems,⁴ it can be assumed that the polymers had vitrified during their cure at the respective temperatures. As the curing temperature is raised, the glass transition region moves to higher temperatures because of the higher crosslink density.^{2-4,25,26} For the samples cured below 110°C, the $\tan \delta$ shows two clear peaks and the modulus exhibits two plateaus. For the sample cured at 110°C, only one transition is apparent; however, the T_g of this material is still less than that obtained for the sample that had been postcured at 160°C. The appearance of two glass transition regions was previously observed in other undercured thermosets^{5,12,13,27,28} and is caused by the recommencement of the curing reaction once the material has gained sufficient molecular mobility during the temperature-ramping DMTA experiment. As a result, when the partly cured sample is heated above its T_g , the increased molecular mobility allows the chemical reaction to recommence, which is reflected by changes in the DMTA trace. For samples cured above 140°C, the DMTA behavior was virtually independent of the cure conditions because this temperature had provided sufficient mobility to allow close to full cure. Assuming that the first peak in $\tan \delta$ is a reasonable approximation of the T_g of the network after the isothermal cure stage, Figure 3 shows the T_g versus the curing temperature (T_{cure}). As found by others,^{4,5,29,30} the T_g is approximately proportional to T_{cure} , until the curing temperature caused complete cure, at which stage the network had reached its maximally attainable T_g . Previous DSC studies of the DGEBA/DDM system⁴ showed that T_g exceeded T_{cure} by about 20°C, whereas Figure 3 shows it to be approximately 40°C. The difference between these values is probably due to the fact that the T_g measured by DSC is lower than that determined at the maximum in $\tan \delta$.³¹

Figure 4 illustrates the dependence of T_g (defined at the $\tan \delta$ maximum) on the conversion for the partly

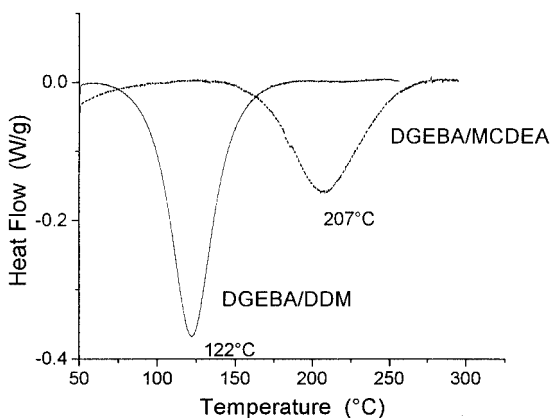


Figure 5 DSC trace (at 2°C/min) of the cure of DGEBA/DDM and DGEBA/MCDEA.

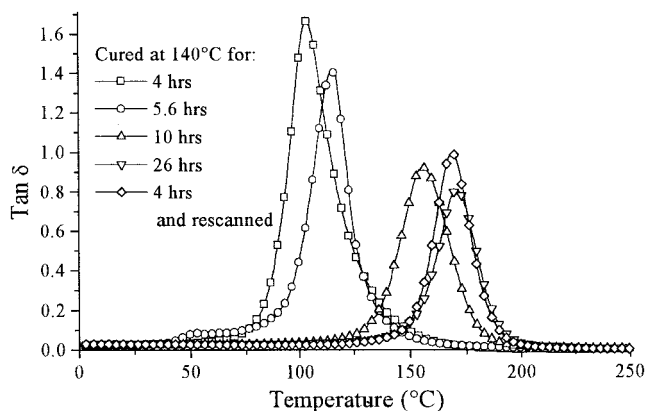


Figure 6 $\tan \delta$ versus temperature for DGEBA/MCDEA cured at differing times at 140°C and for a specimen rescanned after scanning to 250°C. For clarity, not all data points are plotted. The conversions of epoxy groups cured for 4, 5.6, 10, and 26 h before scanning in the DMTA were 67, 72, 89, and 96%, respectively, while it was 95% for the sample cured for 4 h and temperature-ramped in the DMTA.

cured epoxy networks. As expected, the T_g rises as the conversion of the reactive groups increases because the additional crosslinks restrict molecular mobility and the loss of monomer reduces the level of plasticization of the network.

Figures 1 and 2 also show the DMTA behavior of a particular DGEBA/DDM specimen, which had been originally cured at 70°C, but had then been temperature-scanned in the DMTA twice. For this sample, the dynamic mechanical properties on the final scan were close to those of the sample cured at 180°C, suggesting that the sample was close to being fully cured and confirming that the sample polymerizes during the DMTA experiment. In the case of the original sample

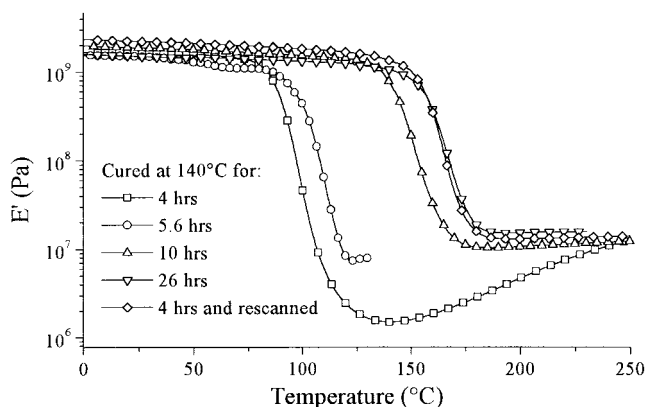


Figure 7 Real modulus for DGEBA/MCDEA cured at differing times at 140°C and for a specimen rescanned after scanning to 250°C. For clarity, not all data points are plotted. The conversions of epoxy groups cured for 4, 5.6, 10, and 26 h before scanning in the DMTA were 67, 72, 89, and 96%, respectively, while it was 95% for the sample cured for 4 h and temperature-ramped in the DMTA.

TABLE I
Breadth of the Glass Transition Region of DGEBA/MCDEA Samples Cured for Various Times to Varying Degrees and of Cured DGEBA/DDM

System	Curing conditions at 140°C	% Conversion	FWHM (°C) from $\tan \delta$	FWHM (°C) from E''	FWHM (°C) from D''
DGEBA/MCDEA	4 h	67	22	20	30
DGEBA/MCDEA	5.6 h	72	18	34	16
DGEBA/MCDEA	10 h	89	25	21	19
DGEBA/MCDEA	26 h	96	20	27	16
DGEBA/MCDEA	4 h and rescanned in DMTA	95	18	23	16
DGEBA/DDM	Cured for 8 h at 160 or 180°C	98	27	20	15

that had only been cured at 70°C, the dynamic data reveal two $\tan \delta$ maxima that are due to continued cure during the thermal DMTA ramp. The DSC cure shown in Figure 5 show that for the DGEBA/DDM system, curing can occur at a high rate in the temperature regime of the DMTA scan. Thus, when the original 70°C-cured sample is scanned in the DMTA, the first peak represents the glass transition of the partially cured network but the subsequent reaction during the temperature scan increases the rigidity of the material, causing a plateau in the modulus curve and the second maximum in $\tan \delta$. Toward the end of the DMTA temperature scans, the rubbery moduli of all of the DGEBA/DDM polymers appear to be relatively independent of the initial curing schedule, suggesting that they have all polymerized to a similar level of cure after temperature scanning in the DMTA. This was confirmed by NIR on the samples after the DMTA run, which showed that the conversion was about 98%. Thus, due to the reaction-induced changes of the dynamic properties in the transition region, it is not possible to use the DGEBA/DDM network system to investigate the dependence of the breadth of the transition region on the extent of reaction per se.

Figures 6 and 7 show the dynamic mechanical properties of DGEBA/MCDEA samples cured for various periods at 140°C. These conditions were based on the isothermal kinetic study by Girard-Reydet et al.¹⁴ and were chosen to give samples with a range of conversions. In contrast to the behavior of DGEBA/DDM, Figure 5 shows that the DGEBA/MCDEA system reacts quite slowly and requires a higher temperature to polymerize at a significant rate, probably due to the electron-withdrawing chloro groups which reduce the nucleophilicity of the amine nitrogen and also due to the steric restrictions of the amine group by the adjacent ethyl groups. As a result, Figures 6 and 7 show that DGEBA/MCDEA exhibits a single glass transition region and it is only after the material is heated to high temperatures (ca. 150°C) in the rubbery region that the curing reaction is able to recommence, causing

the modulus to rise. The DMTA data (Figs. 6 and 7) also show that when the specimen cured at 140°C/4 h was scanned in the DMTA twice, the DMTA data for the second scan were comparable to that of the sample cured for 26 h. At the highest temperatures in the DMTA scan, the rubbery moduli are relatively independent of the initial cure temperature, suggesting that they are all cured to a similar extent.

Table I lists the breadth of the $\tan \delta$ curve (in terms of the FWHM) for the DGEBA/MCDEA samples as a function of cure. It is interesting to note that the breadth of the transition region is relatively independent of the degree of cure of DGEBA/MCDEA, suggesting that crosslink density per se does not cause broadening. Table I also lists the breadth of the transition from the loss modulus (E'') and loss compliance (D''). Although this data are less reliable than the $\tan \delta$ data, because of the potential overlap with sub- T_g relaxation in the case of the E'' data and due to the sensitivity of D'' to small and possibly inaccurate val-

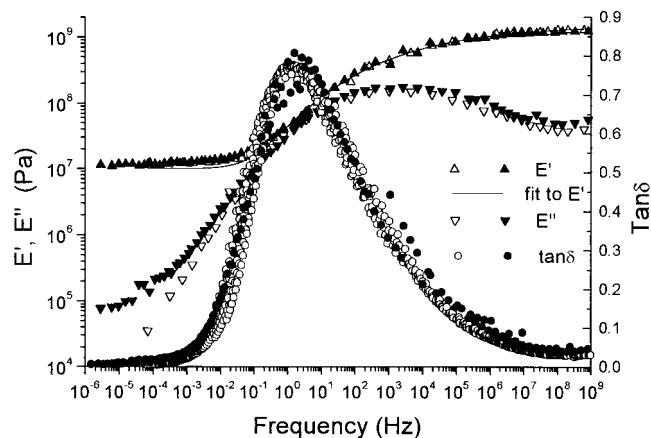


Figure 8 Real and loss modulus and $\tan \delta$ versus frequency for cured DGEBA/MCDEA (duplicate experiments shown) using a reference temperature of 188°C. For clarity, only one or two per four data points are plotted. The solid line shows the fit to the E' data using the stretched exponential.

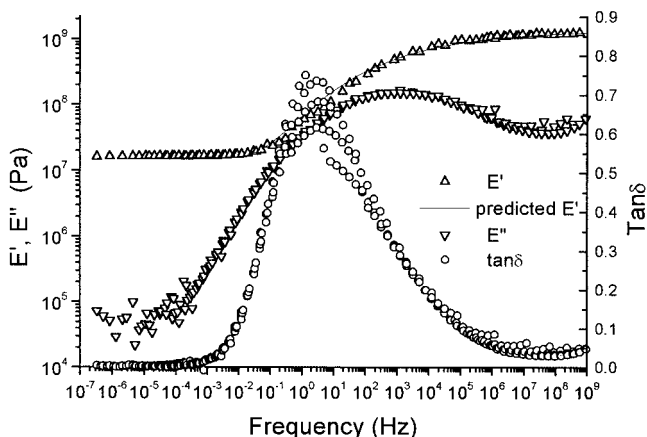


Figure 9 Real and loss modulus and $\tan\delta$ versus frequency for cured DGEBA/DDM using a reference temperature of 168°C. For clarity, only one or two per four data points are plotted. The solid line shows the fit to the E' data using the stretched exponential.

ues of the phase angle, neither show a systematic variation in their breadths. Table I also lists the transition breadth for fully cured DGEBA/DDM and, as expected, this is similar to that of the DGEBA/MCDEA system. However, these transition breadths are quite narrow in comparison to those recently measured by us for cured dimethacrylates¹⁸—for example, in the dimethacrylate systems, the FWHM from the $\tan\delta$ data ranged from 30 to 137°C.

The breadth of the transition in the temperature domain depends on the distribution of relaxation times and the activation energies of the relaxational processes³² and so a comparison of the range of relaxational processes occurring in the glass transition can be obtained more precisely from the variation in the dynamic properties in the frequency domain of the

transition. Figures 8 and 9 show the variations in $\tan\delta$, E' , and E'' with frequency for fully cured samples of DGEBA/DDM and DGEBA/MCDEA. These transitions are considerably narrower than those measured for a series of partially cured dimethacrylate networks.¹⁸ Unfortunately, it was not possible to undertake accurate time–temperature superposition studies with the partially cured versions of the epoxy networks due to the long time required to perform the temperature/frequency sweeps and because of their lack of thermal stability.

Networks formed by chain growth polymerization

DEBPADMA was photocured with the conventional initiator, BEE, at 30 or 50°C for 15 min, causing vitrification of the sample at the curing temperature. The resultant DMTA behavior of these samples is shown in Figure 10. In each case, the data exhibit two $\tan\delta$ maxima and two sigmoidal transitions in the modulus that are similar to those observed above for partly cured DGEBA/DDM systems. Analogously to that discussed above and as previously observed for vinyl ester resins,⁵ this behavior is due to the effect of remobilization of reactive species—in this case, trapped radicals. At the end of the photoirradiation, the polymerization stops but the propagating radicals do not recombine but become trapped in the glassy resin.^{5,13,16,33} When the temperature is subsequently ramped during the DMTA experiment, the sample passes through an initial glass transition whereupon the trapped radicals become active and polymerization recommences in the dark. This additional cure increases the T_g and therefore a second peak is observed in the DMTA experiment. This explanation is confirmed by the data for the DEBPADMA/BEE system, which was initially photocured at 30°C and temperature is scanned in the

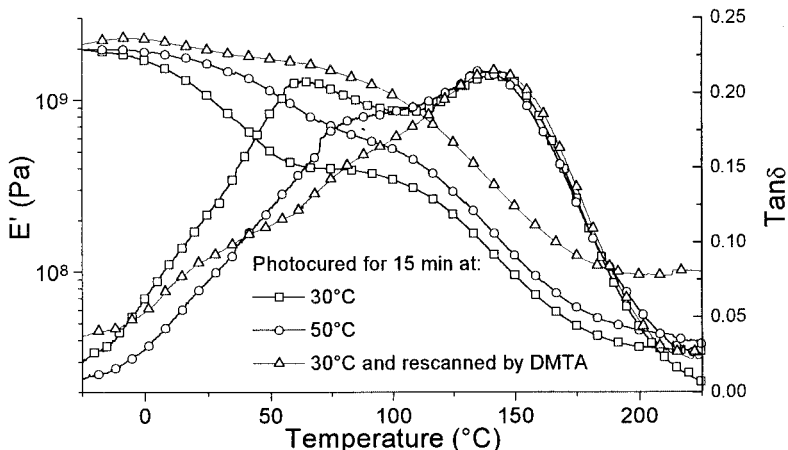


Figure 10 DMTA behavior for DEBPADMA/BEE photocured at 30 or 50°C and the effect of rescanning (up to 250°C) the sample photocured at 30°C on the DMTA properties. For clarity, not all data points are plotted. The conversion of methacrylate groups at the start of each scan was 62, 69, and 83%, respectively.

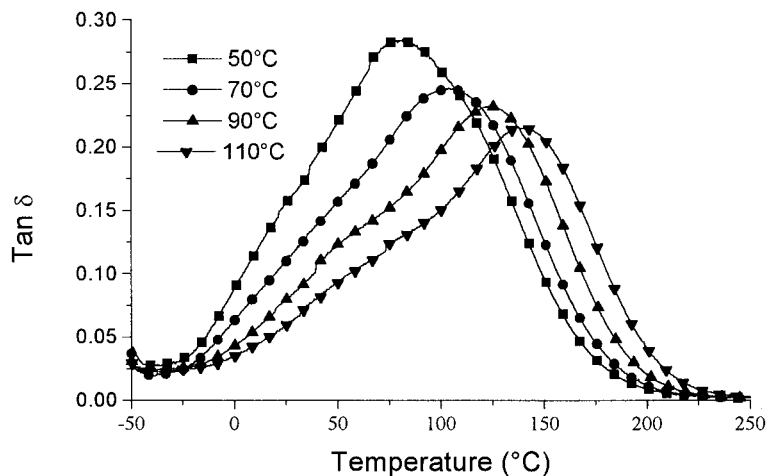


Figure 11 $\tan \delta$ versus temperature for DEBPADMA/XDT photocured for 1 h at the temperatures indicated. For clarity, not all data points are plotted. The methacrylate conversion after photocuring at 50, 70, 90, and 110°C (and after the DMTA scanning, in parentheses) are 57 (57), 65 (73), 70 (70), and 76 (79)%, respectively.

DMTA to 250°C before the final DMTA scan. In the second scan, the lower temperature $\tan \delta$ peak is virtually absent; the modulus shows only a single transition, and the rubbery modulus is higher than that of the other specimens. This behavior is observed because during the first scan, the radicals were reactivated causing further (dark) cure of the resin, which results in the appearance of the two transition regions. However, because no radicals were being produced, most of the radicals eventually underwent bimolecular termination so that, during the second scan, few radicals were present to cause further cure and so only a single transition is observed. The degree of conversion determined before and after the DMTA runs agrees with these results—the conversion of the samples photocured at 30 and 50°C were 62 and 69%,

respectively, but after temperature scanning (to 250°C), the conversion was 83%. The values of the rubbery modulus also agree with this because its value rises in the same order as does the conversion.

In contrast to the DEBPADMA/BEE system, the radicals formed in the DEBPADMA/XDT system terminate shortly after the irradiation ceases because the small and mobile dithiocarbamyl radical, derived from the XDT, is unreactive with monomer but combines with chain radicals when the radiation has ceased, thus preventing further polymerization.^{15–17} The DMTA behavior of the DEBPADMA/XDT system is shown in Figures 11 and 12. For these networks, the material was photocured at various temperatures for 60 min, at which time the material had vitrified. The DMTA data exhibit only one transition region and

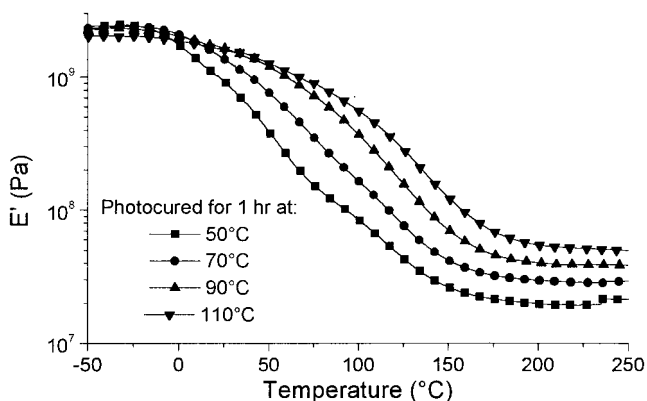


Figure 12 Real modulus versus temperature for DEBPADMA/XDT photocured for 1 h at the temperatures indicated. For clarity, not all data points are plotted. The methacrylate conversion after photocuring at 50, 70, 90, and 110°C (and after the DMTA scanning, in parentheses) are 57 (57), 65 (73), 70 (70) and 76 (79)%, respectively.

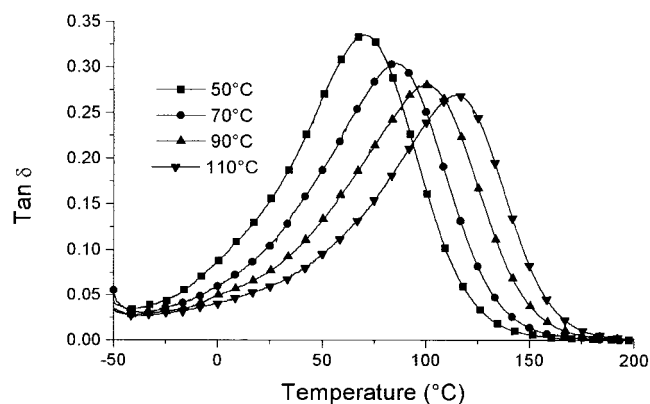


Figure 13 $\tan \delta$ versus temperature for TEBPADMA/XDT photocured for 1 h at the temperatures indicated. For clarity, not all data points are plotted. The methacrylate conversion after photocuring (and after the DMTA scanning, in parentheses) at 50, 70, 90, and 110°C are: 73 (79), 79 (82), 83 (—), and 88 (88)%, respectively.

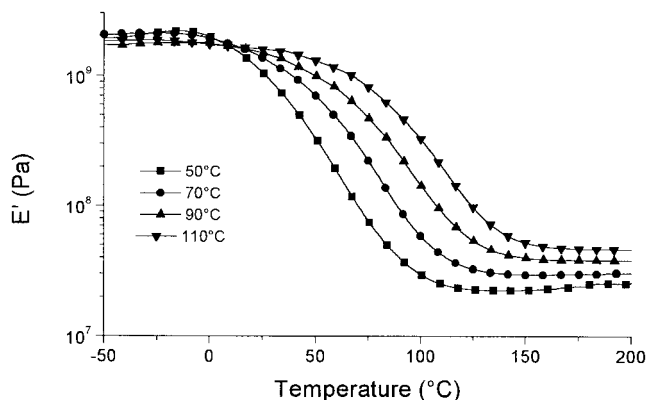


Figure 14 Real modulus versus temperature for TEBPADMA/XDT photocured for 1 h at the temperatures indicated. For clarity, not all data points are plotted. The methacrylate conversion after photocuring (and after the DMTA scanning, in parentheses) at 50, 70, 90, and 110°C are 73 (79), 79 (82), 83 (—), and 88 (88)%, respectively.

NIR analysis shows that the conversion increased by only several percent during the DMTA scan, up to 250°C. It is interesting to note that, contrary to that exhibited by the previously discussed systems, for DEBPADMA/XDT, the modulus in the rubbery region increases as the cure temperature is raised because these networks were cured to differing levels of conversion and they are thermally stable during the DMTA experiment.

Very similar behavior is found when the more flexible TEBPADMA is cured with XDT (Figs. 13 and 14); the $\tan \delta$ and modulus curves display only one transition, the rubbery modulus, and T_g increase with raised conversion and the conversion increases only a few percent during the DMTA scan. As expected of its more flexible backbone structure, the TEBPADMA resin vitrifies at a higher conversion than DEBPADMA when photocured with XDT at the same temperature.

As discussed for the networks cured by step-growth polymerization, Figure 3 shows that there is a simple

relationship between the curing temperature and the glass transition temperature for the DEBPADMA/XDT and TEBPADMA/XDT systems, but surprisingly, the relationship for TEBPADMA/XDT is closer to the 1 : 1 correlation.

As illustrated in Figure 4, the apparent T_g (defined at the $\tan \delta$ maximum) rises with increased conversion of the dimethacrylate networks because the additional crosslinks restrict molecular mobility and the loss of monomer reduces the level of plasticization of the network. For the DEBPADMA system, the nature of the photoinitiator has a significant influence on the apparent T_g because the reaction continues during the DMTA experiment and so the real conversion (and crosslink density) at the glass transition temperature is much higher than it was prior to temperature ramping in the DSC.

Table II lists the breadth of the transition region for partly photocured DEBPADMA/XDT and TEBPADMA/XDT, as determined from the $\tan \delta$. The breadth of the transition region is relatively independent of the degree of cure suggesting that crosslink density per se does not cause broadening. Table II also lists the breadth of the transition from the loss modulus (E'') and loss compliance (D''). Analysis of the transition in terms of the E'' data indicated that the breadth increased with conversion; however, the curves were asymmetric, and this may be associated with the presence of a sub- T_g relaxation, which is overlapped by the glass transition. For the D'' data, the breadth of TEBPADMA is independent of conversion. The DEBPADMA/XDT system has a broader transition for the lowest photocuring temperature; however, this peak also had a lower temperature shoulder. Thus, it appears that the transition breadth is not necessarily broadened by increased conversion, in agreement with the data presented earlier for the DGEBA/MCDEA system. These conclusions are also in agreement with a previous investigation¹⁸ of the glass transition of XDT-photocured networks from nonaethylene glycol dimethacrylate and a 50/50 mix-

TABLE II
Breadth of the Glass Transition Region of DEBPADMA/XDT and TEBPADMA/XDT Samples Cured at Various Temperatures to Varying Degrees of Conversion

System	Curing temperature (°C) for 1 h	% Conversion	FWHM (°C) from $\tan \delta$	FWHM (°C) from E''	FWHM (°C) from D''
DEBPADMA/XDT	50	57	120	77	80
DEBPADMA/XDT	70	65	118	92	68
DEBPADMA/XDT	90	70	120	108	62
DEBPADMA/XDT	110	76	119	134	62
TEBPADMA/XDT	50	71	71	75	47
TEBPADMA/XDT	70	78	75	95	44
TEBPADMA/XDT	90	83	77	102	45
TEBPADMA/XDT	110	88	75	109	43

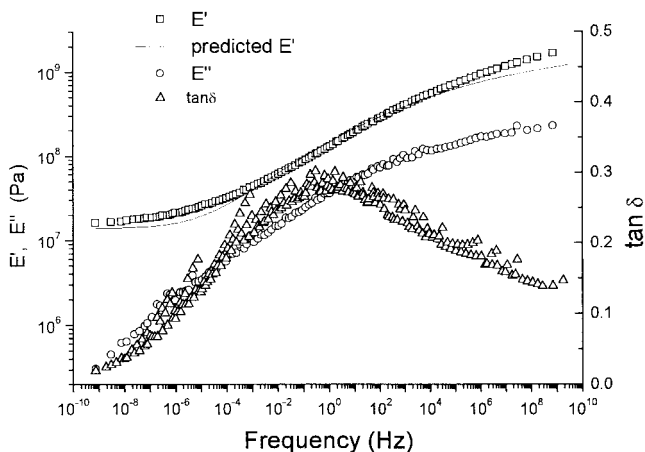


Figure 15 Real and loss modulus and $\tan \delta$ versus frequency for DEBPADM/XDT photocured at 50°C and using a reference temperature of 81°C. For clarity, only one or two per four data points are plotted. The solid line shows the fit to the E' data using the stretched exponential.

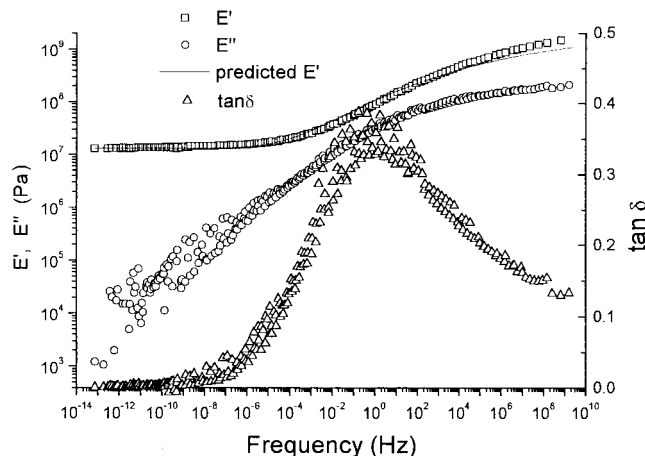


Figure 17 Real and loss modulus and $\tan \delta$ versus frequency for TEBPADM/XDT photocured at 50°C and using a reference temperature of 70°C. For clarity, only one or two per four data points are plotted. The solid line shows the fit to the E' data using the stretched exponential.

ture of phenylglycidyl ether methacrylate and bisphenol-A diglycidyl ether dimethacrylate. However, in this work,¹⁸ the transition region was found to broaden with increased conversion for dimethacrylates with very short (tetraethylene glycol dimethacrylate) or stiff backbones (bisphenol-A diglycidyl ether dimethacrylate).

Figures 15–18 show the variations in $\tan \delta$, E' , and E'' with frequency for partially cured samples of DEBPADMA and TEBPADMA. These transitions are considerably broader than those measured for the epoxy networks (see Figs. 8 and 9) but are similar to dimethacrylate networks previously studied.¹⁸

The breadth of the glass transition regions in the frequency domain of the dimethacrylate and epoxy networks are quantified in Table III in terms of the $\tan \delta$ or D'' data. The breadth of the transition was not determined from the E'' curves because none of those for the dimethacrylates were well-defined on both sides of the transition. As discussed above, the epoxy networks had a much narrower transition region. For the dimethacrylates, the FWHM was relatively independent of conversion but was greater for the more highly crosslinked DEBPADMA networks. The breadth of the transition for the epoxy networks was relatively independent of its structure, perhaps because they have similar crosslink densities.

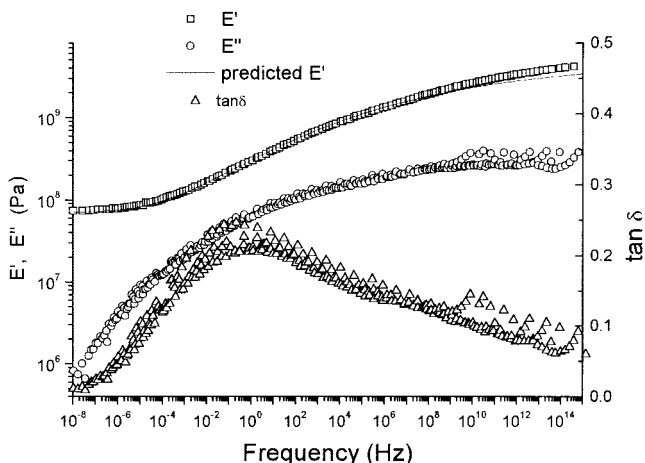


Figure 16 Real and loss modulus and $\tan \delta$ versus frequency for DEBPADM/XDT photocured at 110°C and using a reference temperature of 140°C. For clarity, only one or two per four data points are plotted. The solid line shows the fit to the E' data using the stretched exponential.

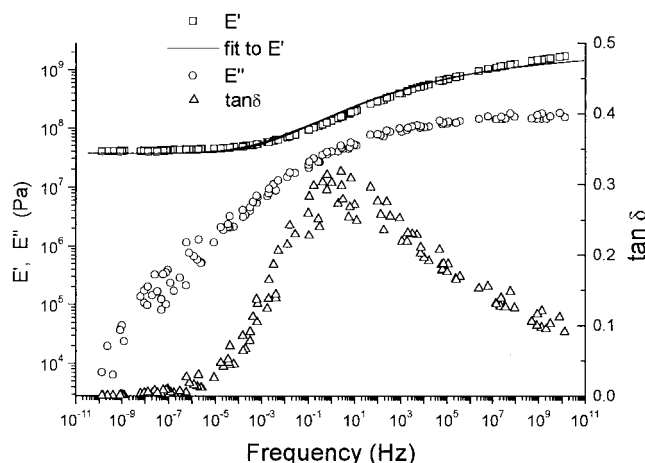


Figure 18 Real and loss modulus and $\tan \delta$ versus frequency for TEBPADM/XDT photocured at 110°C and using a reference temperature of 115°C. For clarity, only one or two per four data points are plotted. The solid line shows the fit to the E' data using the stretched exponential.

TABLE III
WLF and Arrhenius Fitting Parameters to the Shift Factors and the Parameters Obtained
by Fitting the Real Modulus to Exponential Stretch Function

Material and photocuring temperature	T_g (°C) reference temperature	Conversion (%)	FWHM (frequency decades) from $\tan \delta$	FWHM (frequency decades) from D''	Stretched exponential parameters	WLF fitting parameters	Arrhenius activation energy (kJ/mol)
DGEBA/DDM	188	98	3.9	2.2	$n = 0.17$	$C_1 = 13$ $C_2 = 80$	650
DGEBA/MCDEA	168	95	4.0	2.1	$n = 0.16$	$C_1 = 30$ $C_2 = 50$	505
DEBPADMA (50°C)	81	57	13.1	6.3	$n = 0.054$	$C_1 = 160$ $C_2 = 1800$	254
DEBPADMA (110°C)	140	76	14.1	6.1	$n = 0.058$	$C_1 = 40$ $C_2 = 435$	315
TEBPADMA (50°C)	70	73	10.5	5.5	$n = 0.063$	$C_1 = 52$ $C_2 = 387$	299
TEBPADMA (110°C)	115	88	10.2	5.1	$n = 0.080$	$C_1 = 39$ $C_2 = 297$	364

The real modulus data were fitted to the stretched exponential [eq. (2)] to obtain an alternative measure of the breadth of the transition region. The values of the distribution parameter (n) are listed in Table III. In contrast to that found with linear polymers,²⁴ where the distribution parameter is often close to 0.5, Table III shows that for the dimethacrylates, n ranges from 0.05 to 0.08, suggesting a much wider range of relaxation times. These results are similar to those obtained in our previous work¹⁸ on dimethacrylates and those also measured by Kannurpatti et al.^{10,13} by DMTA of related methacrylate networks. Surprisingly, the distribution parameter appears to rise with increased conversion but the change is small. In our previous study,¹⁸ no clear correlation with either the structure or the crosslink density of the dimethacrylates with the distribution parameter was obvious. Both of the epoxy resins have similar distribution parameters and they are considerably higher than for the dimethacrylates, indicating a narrower range of molecular motions associated with the glass transition.

Table III also lists the parameters obtained by frequency-temperature shifting of the multifrequency data. The WLF expression [eq. (1)] was fitted to the shift parameters for the dimethacrylate resins but the fits were relatively poor (with R^2 values as low as 0.5) and some of the parameters were quite unrealistic given that the universal values are 16 and 50°C for C_1 and C_2 , respectively.²² In contrast, for the fully cured epoxy networks, the WLF equation fitted the shift factors well with R^2 values between 0.97 and 0.99 and the values of C_1 and C_2 are more reasonable. The shift parameters were also fitted to the Arrhenius equation and gave R^2 values above 0.99 for the DEBPADMA and TEBPADMA resins and of 0.98 for the epoxy networks. The activation energies for the epoxy networks is of the order of 500–600 kJ/mol and this is

lower than the values of 700–900 kJ/mol obtained by Cao et al.,³ but is higher than the values of 200 kJ/mol obtained by Ilavsky et al.³⁴ for similar networks. The activation energies of the dimethacrylates were of the order of 250–350 kJ/mol, which are much lower than the epoxy resins, suggesting the barrier to segmental motion associated with the glass transition is lower for the dimethacrylates. These values are similar to the DMTA values reported by Forrest³⁵ (220–286 kJ/mol) on related dimethacrylates but are a little higher than that reported by Dargent et al.³⁶ (168–188 kJ/mol) by using thermally stimulated depolarization current analysis on an unidentified dimethacrylate. For both DEBPADMA and TEBPADMA, the activation energy rises with conversion, suggesting the barrier to large-scale segmental motion increases with higher crosslink density; however, the opposite effect was found by Dargent et al.³⁶

CONCLUSION

The advantage of using partly reacted but thermally stable networks in probing the glass transition region was demonstrated by contrasting the viscoelastic behavior of amine-cured epoxies and photoinitiated cured dimethacrylates. Both of the epoxy networks recommenced polymerization in either the transition or the rubbery region, which resulted in either the occurrence of two transitions in the modulus and $\tan \delta$ trace (for DGEBA/DDM) or a rapid and substantial rise (for DGEBA/MCDEA) in the modulus in the rubbery region. In contrast, the XDT-photoinitiated dimethacrylates underwent only small amounts of additional cure (and at very high temperatures) during the DMTA experiment.

For networks isothermally cured until vitrification, the temperature of the first (or only) $\tan \delta$ peak in the

glass transition region was correlated with the curing temperature because devitrification commences just above the initial curing temperature until the sample is fully cured. The T_g was also correlated with the degree of cure due to the effect of crosslinks on reducing molecular mobility and of the loss of plasticizing species.

The viscoelastic properties were analyzed by time-temperature supposition and the shift factors fitted to the WLF and Arrhenius expressions. The WLF parameters fitted to the data for the epoxy networks were similar to the universal values but those for the dimethacrylates were not very close. The Arrhenius activation energies were higher for the epoxy networks than for the dimethacrylates.

The breadth of the glass transition in the temperature domain, as measured by the $\tan \delta$ and D'' (and in some cases the E'') data, did not show significant dependence on the level of cure of either the epoxy or the dimethacrylate resins but the dimethacrylate networks had considerably broader transitions than did the epoxy networks. These conclusions were confirmed by measurements of the transition breadth in the frequency domain and also from analysis of the modulus data in terms of the stretched exponential expression. This suggests that, for the systems studied, crosslinking does not broaden the glass transition per se.

The authors thank Prof. Chris Bowman (University of Colorado) for stimulating discussions in this area.

References

- Pascault, J. -P.; Sautereau, H.; Verdu, J.; Williams, R. J. J. *Thermosetting Polymers*; Marcel Dekker: New York, 2002.
- Aronhime, M.; Gillham, J. *Adv Polym Sci* 1986, 78, 83.
- Cao, Z.; Galy, J.; Gerard, J. F.; Sautereau, H. *Polym Networks Blends* 1993, 4, 15.
- Wise, C. W.; Cook, W. D.; Goodwin, A. A. *Polymer* 1997, 38, 3251.
- Cook, W. D.; Simon, G. P.; Burchill, P. J.; Lau, M.; Fitch, T. J. *J Appl Polym Sci* 1997, 64, 769.
- Scott, T. F.; Cook, W. D.; Forsythe, J. S.; *Polymer*, 2002, 43, 5839.
- Dusek, K. *Angew Makromol Chem* 1996, 240, 1.
- Nielsen, L.; *Macromol J. Sci, Rev Macromol Chem* 1969, C3, 69.
- Simon, G. P.; Allen, P. E. M.; Williams, D. R. G. *Polymer* 1991, 32, 2577.
- Kannurpatti, A. R.; Anseth, J. W.; Bowman, C. N. *Polymer* 1998, 39, 2507.
- Young, J. S.; Bowman, C. N. *Macromolecules* 1999, 32, 6073.
- Wisnarakitt G.; Gillham, J. K. J. *J Appl Polym Sci* 1991, 42, 2453.
- Kannurpatti, A. R.; Anderson, K. J.; Anseth, J. W.; Bowman, C. N. *J Polym Sci Part B: Polym Phys* 1997, 35, 2297.
- Girard-Reydet, E.; Richardi, C. C.; Sautereau, H.; Pascault, J. P. *Macromolecules* 1995, 28, 7599.
- Otsu T.; Yoshida, M. *Makromol Chem Rapid Commun* 1982, 3, 127.
- Kannurpatti, A. R.; Lu, S.; Bunker, G. M.; Bowman, C. N. *Macromolecules* 1996, 29, 7310.
- Moad G.; Solomon, D. H. *The Chemistry of Free Radical Polymerization*; Pergamon: Oxford, 1995.
- Cook, W. D.; Forsythe, J. S.; Irawati, N.; Scott, T. F.; Xia, W. Z. *J Appl Polym Sci* 2003, 90, 3753.
- Otsu T.; Kuriyama, A. *Polym Bull* 1984, 11, 135.
- Rey, L.; Galy, J.; Sautereau, H. *Macromolecules* 2000, 33, 6780.
- Lachenal, G.; Pierre, A.; Poisson, N. *Micron* 1996, 27, 329.
- Ferry, J. D. *Viscoelastic Properties of Polymers*; Wiley: New York, 1970.
- Williams G.; Watts, D. C. *Trans Faraday Soc* 1971, 67, 1323.
- Matsuoka, S. *Relaxation Phenomena in Polymers*; Hanser: Munich, 1992.
- Pascault J. P.; Williams, R. J. J. *J Polym Sci, Part B: Polym Phys* 1990, 28, 85.
- Hale, A.; Macosko, C. W.; Bair, H. E. *Macromolecules* 1991, 24, 2610.
- Gillham, J. K.; Benci, J. A. *J Appl Polym Sci* 1974, 18, 951.
- Enns, J. B.; Gillham, K. K. *J Appl Polym Sci* 1983, 28, 2567.
- Wisnarakitt, G.; Gillham, J. K. *J Appl Polym Sci* 1990, 41, 2885.
- Tungare, A. V.; Martin, G. C. *Polym Eng Sci* 1993, 33, 614.
- Nielsen, L. E.; Landel, R. F. *Mechanical Properties of Polymers and Composites*; Marcel Dekker: New York, 1974; Chapter 4.
- McCrum, N. G.; Read, B. E.; Williams, G. *Anelastic and Dielectric Effects in Solid Polymers*, Dover; New York, 1967.
- Kloosterboer, J. G. *Adv Polym Sci* 1988, 84, 1.
- Ilavsky, M.; Zelenka, J.; Spacek, V.; Dusek, K. *Polym Networks Blends* 1992, 2, 95.
- Forrest, M. *The Development and Characterisation of Novel Ternary-Phase Dental Composites for Improved Toughness*, PhD thesis, Monash University, 2001.
- Dargent, E.; Kattan, M.; Cabot, C.; Lebaudy, P.; Ledru, J.; Grenet, J. *J Appl Polym Sci* 1999, 74, 2716.